

## Enhanced adsorptive removal of methylene blue by low-temperature biochar derived from municipal activated sludge

Weisheng Chen<sup>a,b</sup>, Yiping Guo<sup>a,b</sup>, Xiao Mi<sup>a,b</sup>, Yang Yu<sup>c</sup>, Guoting Li<sup>a,b,\*</sup>

<sup>a</sup>Department of Environmental and Municipal Engineering, North China University of Water Resources and Electric Power, Zhengzhou 450011, China, Tel. +86-371-69127436/+86-371-69127538; Fax: +86-371-65790239; emails: lipsonny@163.com (G. Li), tclbaby@126.com (W. Chen), guoyiping@ncwu.edu.cn (Y. Guo), mixiao@ncwu.edu.cn (X. Mi)

<sup>b</sup>Henan Key Laboratory of Water Environment Simulation and Treatment, North China University of Water Resources and Electric Power, Zhengzhou 450011, China

<sup>c</sup>Guangdong Key Laboratory of Environmental Pollution and Health, and School of Environment, Jinan University, Guangzhou 510632, China, email: yuyang@jnu.edu.cn (Y. Yu)

Received 30 June 2019; Accepted 14 January 2020

### ABSTRACT

Low-temperature biochar was prepared by pyrolyzing municipal waste activated sludge and used for the adsorptive removal of a cationic dye methylene blue (MB). It was observed that both the as-prepared and demineralized sludge biochars pyrolyzed at 200°C (BC200) outperformed other biochars for MB uptake. The sophisticated pore structure and suitable surface properties of sludge biochar BC200 might facilitate the uptake of MB, in which the abundant surface functional groups played the key role. The uptake of MB on both as-prepared and demineralized BC200 increased dramatically from pH 5, while the demineralized BC200 performed better than the as-prepared BC200 at pH  $\geq 7$ . The experimental data was better fitted by the pseudo-second-order model, indicating a possible chemisorption process. The Langmuir model worked better to describe the isotherm data than Freundlich model for both the as-prepared and demineralized BC200, suggesting a monolayer coverage of MB on both biochars. At 298 K, the  $q_m$  values for the as-prepared and demineralized BC200 were 177.6 and 184.9 mg/g, respectively, much higher than those of other biochars reported in literature. The demineralized BC200 had an almost equivalent adsorption capability to the as-prepared BC200.

**Keywords:** Low-temperature biochar; Activated sludge; Methylene blue; Adsorption; Kinetics; Isotherm

### 1. Introduction

As one of the physical-chemical methods for water treatment, adsorption technology has attracted increasing concern because of its excellent removal capacity for various pollutants from aqueous solutions. Especially for the removal of anionic pollutants, adsorption shows its priority to other techniques with the advantages of high efficiency, low cost, ease of operation and low sensitivity to other co-existing substances [1,2]. Activated carbon, which was first used by the ancient Egyptians in 2000 B.C, is still

widely applied in water treatments. However, the application of commercial activated carbon is limited as a consequence of complicated production technology and higher costs. Therefore, the development of low-cost carbon-based adsorbents, including low production and application cost, is highly anticipated.

Although some biomasses can be directly used as low-cost adsorbents, biochars derived from biomasses such as agricultural wastes, forestry wastes, animal manures and activated sludge via incomplete combustion operations such as pyrolysis and carbonization, are considered as ideal

\* Corresponding author.

substitution of activated carbon in the field of water treatment [3–8]. Compared to the direct application of the above biomasses, biochar will cause neglectable secondary pollution and work as an eco-friendly adsorbent for soil and water contaminated with organic/inorganic substances. Furthermore, the generation of biochar offers the chance to turn bioenergy into a carbon-negative industry as low-temperature pyrolysis, with carbon sequestration and gas capture, is expected to be a carbon-neutral energy source [9,10]. Currently, low-temperature pyrolysis is conveniently applied to convert biomass into biochars [11] in which organic leaching and secondary pollution from the raw biomass can be effectively avoided. As one of the typical municipal wastes, a huge amount of sludge is generated from biological wastewater treatment annually, which would pose a severe threat to environment and human health if they are improperly treated and disposed of. Activated sludge itself has the potential for wastewater treatment. For instance, anaerobic granular sludge has advantages of lower energy consumption, higher loading, and less amount of residual sludge, especially when treating a high concentration of organic wastewater [12]. However, as sludge contains lots of bacteria, protozoa, and extracellular polymeric substances, direct use of sludge for wastewater treatment is a risk under some circumstances. Comparatively speaking, utilization of sludge biochar might be an ideal choice for practical adsorption process.

Further, the pyrolytic temperature is one of the key parameters to determine the adsorption capability of generated biochars. The increased pyrolytic temperature could increase the carbon content, improve thermal stability and regulate the structural, and surface, characteristics of biochars [13,14]. Our previous study indicated that wheat straw biochar pyrolyzed at 200°C was more sensitive to an external magnetic field due to its unique surface structure [15]. Therefore, the uptake of contaminants is expected to be significantly influenced by the pyrolytic temperature. In this study, sludge biochars were prepared under different pyrolytic temperature and the adsorption of the cationic dye methylene blue (MB) on the prepared biochars were evaluated by a series of batch experiments, including effects of the pyrolytic temperature of biochar generation, solution pH and initial dye concentration, adsorption kinetics and isotherm. The adsorption mechanism was further discussed. What should be mentioned is that the exhausted adsorbent could be regenerated by thermal treatment for reuse or subjected for incineration as a kind of industrial waste.

## 2. Materials and methods

### 2.1. Materials

MB (purity > 98.5%,) was purchased from Tianjin Chemical Reagent Research Institute (Tianjin, China). The other chemicals used were of analytical grade. Deionized (DI) water was used to prepare solutions throughout the study.

### 2.2. Preparation of biochars derived from activated sludge

Municipal activated sludge was collected from the dewatering stage of Matougang wastewater treatment plant (Zhengzhou City, China). The collected sludge was air-dried,

ground and screened through a 40 mesh sieve for further use. The pre-treated sludge was put into a crucible, in a compressed state, and covered with a tight-fitting lid. Then, the crucible was placed in a muffle furnace under various temperatures (200°C, 300°C, 400°C, 500°C, and 600°C) for 2 h. After natural cooling, the resultant sludge biochar was placed in a 4 mol/L HCl solution for 12 h and separated by filtration. After that, the residues were rinsed with DI water until a neutral solution pH was achieved. The product was then oven-dried overnight at 80°C. The treated biochars were finally preserved in a desiccator for subsequent use. These sludge biochars were hereafter designated as BC200, BC300, BC400, BC500, and BC600, respectively wherein the suffix number represented the pyrolytic temperature.

### 2.3. Characterization

The surface morphologies of the raw sludge and biochars pyrolyzed at different temperatures were characterized by a Philips Quanta-2000 scanning electron microscopy (SEM) coupled with an energy-dispersive X-ray (EDX) spectrometer (Holland). Surface functional groups of these biochars were recorded on a Nicolet NEXUS 470 Fourier-transform infrared spectroscopy (FTIR) spectrophotometer from 400 to 4,000  $\text{cm}^{-1}$ . The specific surface areas of sludge biochars were measured by nitrogen adsorption/desorption using BET method with a surface area and pore size analyzer (NOVA 2200e, USA).

### 2.4. Batch adsorption studies

Adsorption of MB onto the sludge biochars were conducted in cylindrical flasks. The stock solutions of MB (500 mg/L) were prepared by dissolving MB in DI water. All working solutions with the desired concentration were prepared by diluting the stock solution with DI water. 10 mg of sludge biochar was added to a conical flask containing 50 mL 10 mg/L of MB solution. Constant and vigorous stirring was maintained by mechanical agitation for 24 h. For the kinetics study, 200 mg of sludge biochar was added to a 1,000 mL solution with the initial MB concentration of 20 mg/L. The mixed solution was magnetically stirred at a constant rate.

After adsorption, samples were collected and filtered through a 0.45  $\mu\text{m}$  syringe membrane before analysis. The adsorption reaction was carried out at 298 K except for the study on the effect of reaction temperature on the isotherm. All solution pH values were maintained at neutral pH except for the study of pH effect. Solution pH adjustment was adjusted by the addition of a dilute HCl or NaOH solution.

### 2.5. Analysis methods

The concentration of MB was analysed using an UVmini-1240 spectrophotometer (Shimadzu, Japan) by monitoring emissions at the wavelength of maximum absorption (664 nm). The removal percentage of MB was given by:

$$R = \left( 1 - \frac{C_t}{C_0} \right) \times 100\% \quad (1)$$

The adsorption capacities ( $q_e$ ,  $q_t$ ) were calculated as follows:

$$q_e = (C_0 - C_e) \frac{V}{W} \quad (2)$$

$$q_t = (C_0 - C_t) \frac{V}{W} \quad (3)$$

where  $q_e$  and  $q_t$  (mg/g) are the adsorption capacities at equilibrium and time  $t$  (minutes);  $C_0$ ,  $C_e$  and  $C_t$  (mg/L) are the concentrations of MB at initial stage, equilibrium and  $t$  (minutes), respectively;  $V$  (L) is the volume of solution, and  $W$  (g) is the mass of the sludge biochar used.

### 3. Results and discussion

#### 3.1. Characterization of sludge biochars

##### 3.1.1. Surface morphology

The surface morphologies of the raw sludge, demineralized BC200, B300, and BC400 are shown in Fig. 1. Typically, the raw sludge was severely compacted while the sludge biochars consisted of particles with the diameters below 10  $\mu\text{m}$ . After pyrolysis, the resulting biochars had a loose and porous structure. Moreover, the particle size of biochar was significantly decreased with an increase in pyrolysis temperature. For the BC400 biochar, the particle size actually became less than 1  $\mu\text{m}$ , in which the biochar

evidently had an abundant pore structure compared to other biochars. The porous structure of sludge biochar was expected to facilitate the uptake of contaminants from aqueous solution.

From EDX analysis, carbon contents of the raw sludge, demineralized BC200, BC300 and BC400 were 50.8%, 53.0%, 54.5%, and 55.9% (wt.%), respectively. Obviously, both the raw sludge and related biochars are carbon-rich, and carbon content increased with the pyrolysis temperature slowly. After pyrolysis, the oxygen content decreased sharply from 37.8% of the raw sludge to 4.9% of demineralized BC200, which was similar to the pyrolysis performance of other waste [16]. Interestingly, the nitrogen content increased from 0% of the raw sludge to 3.3% of demineralized BC200. Like biochars derived from other wastes, the surface of the prepared biochars would become more hydrophobic due to the increased carbon content and the concurrent decrease in oxygen content with an increase in pyrolytic temperature.

##### 3.1.2. Fourier-transform infrared spectroscopy

The FTIR spectra of the raw sludge biochars BC200, BC300 and BC400 are compared in Fig. 2. Typically, the strong band at 3,429  $\text{cm}^{-1}$  represented the stretching vibration of adsorbed water. This band almost disappeared when the pyrolytic temperature was higher than 200°C. The bands at 2,920 and 2,851  $\text{cm}^{-1}$  were assigned to C–H stretching, which weakened gradually as well. These indicated the significant loss of moisture, water of hydration and C–H functional groups during the pyrolysis process. Meanwhile,

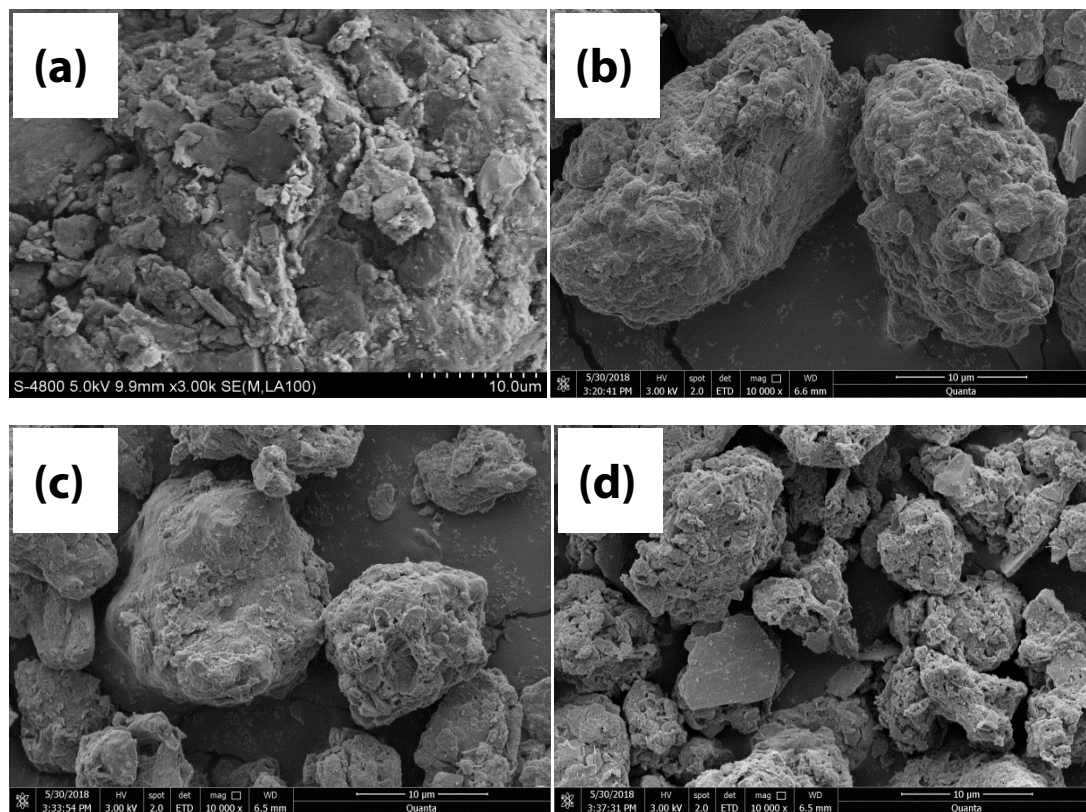


Fig. 1. SEM micrographs of the raw sludge (a), and demineralized sludge biochars including BC200 (b), BC300 (c) and BC400 (d).

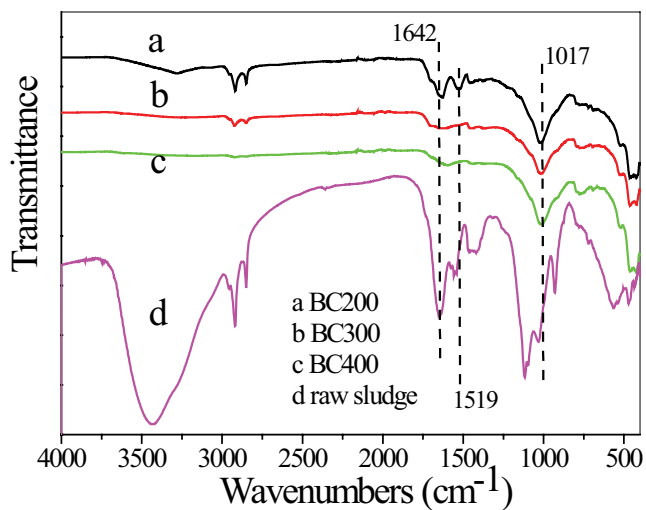


Fig. 2. FTIR spectra of the raw sludge and the sludge biochar BC200, BC300 and BC400.

the bands of the raw sludge at  $929\text{ cm}^{-1}$ ,  $1,417\text{ cm}^{-1}$  ( $-\text{CH}_2$  or  $\text{C}=\text{C}$ ) and  $1,642\text{ cm}^{-1}$  (aromatic  $\text{C}=\text{C}$  and  $\text{C}=\text{O}$ ) almost disappeared [12,17,18], while the band at  $1,030\text{ cm}^{-1}$  ( $\text{C}-\text{C}$  and  $\text{C}-\text{O}$  in esters) shifted to  $1,017\text{ cm}^{-1}$ . Further, among all the biochars including BC200, BC300 and BC 400, the total FTIR absorption bands on BC200 were typically more well-defined and stronger, indicating more abundant functional groups of BC200 surface. It was worth to mention that the band at  $1,519\text{ cm}^{-1}$  was attributed to the vibration of  $\text{NH}$ -groups [12], which was only well-defined in the FTIR spectra of BC200. The loss of oxygen-containing functional groups such as carbonyl and hydroxyl groups indicated the decline of oxygen content with increasing in pyrolytic temperature, which was consistent with the afore-mentioned EDX observations.

### 3.2. Effect of pyrolytic temperature of biochars on MB adsorption

The pyrolytic temperature of biochar can influence its surface structure as well as surface chemical properties such as contents of O- and H-containing functional groups [5]. The resulting surface polarity, surface area, and aromaticity are important characteristics affecting the adsorption of organic contaminants [19]. Considering the definite organic leaching and secondary pollution caused by the raw sludge, only the sludge biochars were applied for MB adsorption. Therefore, the adsorption performance of the as-prepared and demineralized biochars BC200, BC300, BC400, BC500, and BC600 were compared and the results are presented in Fig. 3. The as-prepared and demineralized biochars BC200 outperformed other biochars for the uptake of MB. The uptake of MB by the as-prepared and demineralized BC200 achieved as much as  $47.0$  and  $49.2\text{ mg/g}$ , respectively. The corresponding removal percentages were  $94.0\%$  and  $98.4\%$ , respectively. As mentioned above, the abundant  $\text{NH}$ - groups were observed on BC200 alone judged from the FTIR spectra of these biochars, which is consistent with the afore-mentioned EDX results. It was reported that the presence of N-containing groups could be favorable for adsorption of MB through

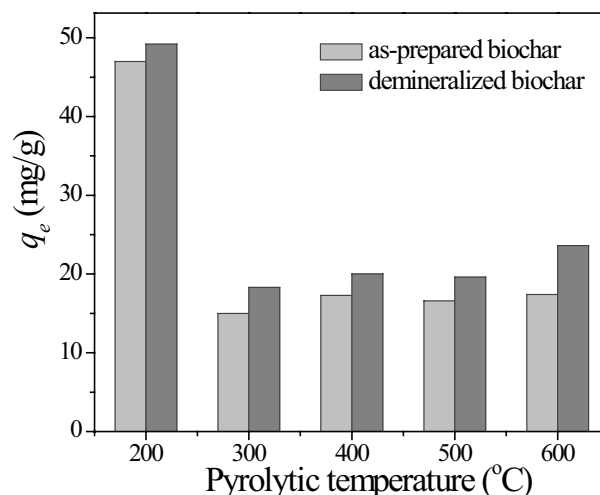


Fig. 3. Effect of pyrolytic temperature of biochar on MB adsorption. MB concentration was  $10\text{ mg/L}$ .

strong  $\pi-\pi$  electron donation-acceptance interaction with N-containing aromatic structure [20]. Considering the abundant functional groups on BC200, it could be deduced that it was the superior surface functional groups on BC200 that led to an enhanced adsorption capability for MB. Though the carbon content of the demineralized BC200 was higher than that of the as-prepared biochar, the difference between the two biochars was not significant in this case. An increase in pyrolytic temperature usually increases the surface areas of biochars, which is beneficial to the MB adsorption. The surface areas of BC200, BC400, and BC600 were  $0.8$ ,  $6.4$ , and  $51.7\text{ m}^2/\text{g}$ , respectively. Unfortunately, the uptake of MB on BC600 was not the highest among these biochars. The low adsorption capability of MB on BC600 indicated that the surface chemical property of biochar played a more important role during the adsorption of MB. Additionally, as the yield for BC200 production achieved as much as  $52.3\%$ , which was especially higher than those of other biochars, BC200 was the best choice for contaminant adsorption. Therefore, both the as-prepared and demineralized BC200 was selected in the following tests.

### 3.3. Effect of MB concentration on adsorption

The effect of MB concentration on the adsorption performance was investigated to further figure out the adsorption capability of the as-prepared and demineralized biochars BC200, as illustrated in Fig. 4. For the demineralized BC200, The adsorption capacity for MB ( $q_e$ ) at initial MB concentration of  $5$ ,  $10$ ,  $20$  and  $40\text{ mg/L}$  can reach  $24.8$ ,  $49.2$ ,  $74.0$  and  $94.3\text{ mg/g}$ , respectively. Accordingly, the corresponding removal percentages were of  $99.6\%$ ,  $98.4\%$ ,  $68.2\%$  and  $48.5\%$ , respectively. Owing to the higher carbon content of the demineralized BC200, a slightly higher MB uptake was observed at different initial MB concentrations. Additionally, the residual MB solution was almost colorless at an initial MB concentration of  $5$  and  $10\text{ mg/L}$ . As such, only a very limited amount of the sludge biochar BC200 can achieve the decolorization and effective removal of MB from water,

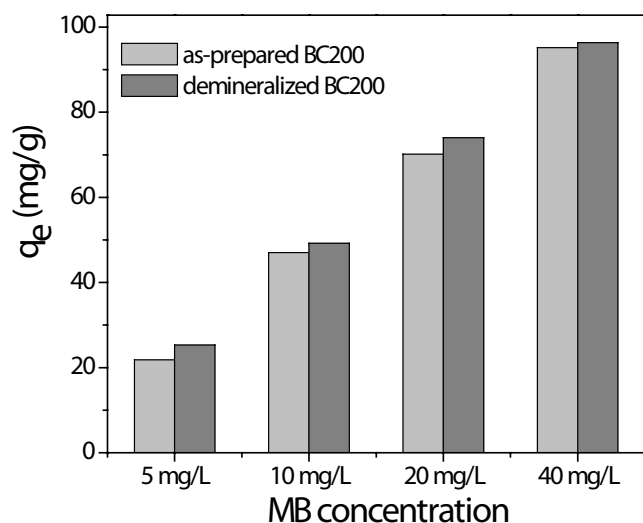


Fig. 4. Effect of MB concentration on the adsorption performance.

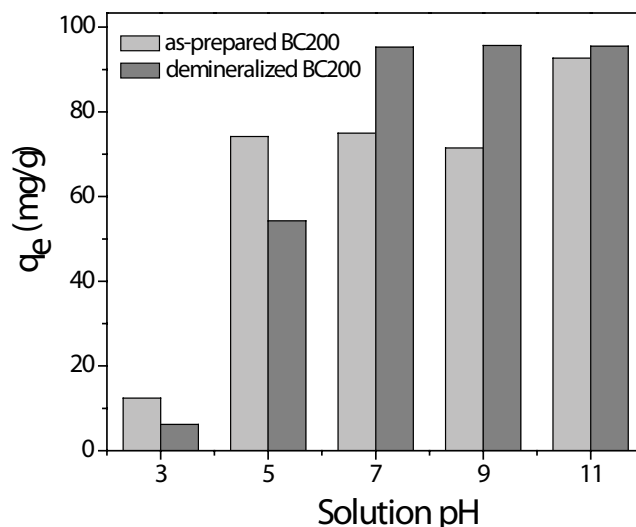


Fig. 5. Effect of solution pH on MB adsorption. MB concentration was 20 mg/L.

suggesting a promising application potential of sludge biochar on treating the dye wastewater.

### 3.4. Effect of solution pH

As well known, the protonation of functional groups on the adsorbent can be highly affected by the solution pH. Therefore, the effect of solution pH on the adsorption of MB on sludge biochar BC200 was investigated and results are shown in Fig. 5. The uptake of MB on the as-prepared BC200 was increased dramatically when pH was evaluated from 3.0 to 5.0, turn into a plateau in the pH range of 5.0–9.0 and further increased at extremely basic pH 11.0. For the demineralized BC200, the adsorption of MB was enhanced when pH was increased from 3.0 to 7.0 and kept stable with the further increase in the solution pH. At high solution pH, the deprotonation of functional groups (e.g., O<sup>-</sup>) on the biochar surface would cause that the surface charge of biochar become more negatively-charged which was beneficial to the adsorption of positively-charged MB molecules because of the enhancement of their electrostatic attraction force. As such, the adsorption of water-soluble MB on both the as-prepared and demineralized BC200 was highly pH-dependent, indicating the extreme importance of surface functional groups.

On the other hand, it was reported that the ash and fixed carbon contents were 55.7%, and 4.6%, respectively in the sewage sludge sample, while 65.8% and 6.8%, respectively in the sewage sludge pyrolyzed at 300°C [18]. The role of ash might play a fundamental role in the uptake of MB molecules, while the fixed carbon would more highly affect the adsorption performance of biochar under different solution pH due to strong sensitivity toward pH of functional groups on the surface of fixed carbon. The better adsorption performance of the demineralized BC200 at pH ≥ 7 might be attributed to the higher adsorption capability of the fixed carbon than the ash within the biochar BC200. By contrast, under acidic conditions, the abundant fixed carbon

led to the demineralized BC200 more positively charged than the ash surface, and the strong repulsive force on the demineralized BC200 might have inhibited the MB uptake significantly. Furthermore, considering the expenditure for biochar demineralization, the direct use of the as-prepared sludge biochar might be an optimal choice for the adsorptive removal of organic contaminants.

### 3.5. Adsorption kinetics

Adsorption kinetics study could predict adsorption rates and understand adsorption mechanism of an adsorbent. The adsorption kinetics of MB onto the biochar BC200 was investigated at pH 3.0, 5.0, 7.0, 9.0 and 11.0, respectively. Typical kinetics models, including the Elovich, the pseudo-first-order, and pseudo-second-order models were used to fit the experimental data.

The Elovich model, which is used to describe chemisorption occurring on a solid-liquid interface, can be expressed as [21,22]:

$$q_t = k \ln(t) + a \quad (4)$$

where  $a$  (g mg/min) and  $k$  (mg/g) are constants.

The nonlinear and linear pseudo-first-order model is expressed as [23]:

$$q_t = q_e (1 - e^{-k_1 t}) \quad (5)$$

$$\ln(q_e - q_t) = \ln q_e - k_1 t \quad (6)$$

The nonlinear and linear pseudo-second-order model can be expressed as [24]:

$$q_t = \frac{k_2 q_e^2 t}{(1 + k_2 q_e t)} \quad (7)$$

$$\frac{t}{q_t} = \frac{1}{k_2 q_e^2} + \frac{t}{q_e} \quad (8)$$

where  $q_e$  and  $q_t$  are the adsorption capacities (mg/g) of the biochar at equilibrium and at time  $t$  (min), respectively;  $k_1$  ( $\text{min}^{-1}$ ) and  $k_2$  ( $\text{g}/(\text{mg min})$ ) are the related adsorption rate constant for the pseudo-first-order and pseudo-second-order model, respectively.

The kinetics data at neutral solution pH 7.0 and the fitting results by the three kinetic models are as illustrated in Fig. 6. As to the linear pseudo-first-order and pseudo-second-order kinetics models, they are simulated kinetic parameters for both the as-prepared and demineralized BC200 under different pH conditions are listed in Table 1. The determined coefficients ( $R^2$ ) of the linear pseudo-second-order kinetics model were all above 0.960, which were especially higher than those of the linear pseudo-first-order model. The calculated  $q_e$  values were much close to the experimental values using the pseudo-second-order kinetics model as well. For instance, the  $q_e$  value of the demineralized BC200 at pH 7.0 was 96.6 mg/g by the linear

pseudo-second-order kinetics model, which was much close to the experimental value 95.5 mg/g. Apparently, the linear pseudo-second-order kinetics model fitted the experimental data better. As such, it can be deduced that MB uptake on both BC200 and demineralized BC200 was controlled by a chemisorption process.

Meanwhile, from Fig. 6c, it can be observed that about 70.3% and 88.1% of the total MB molecules were respectively adsorbed on as-prepared and demineralized biochar within the initial 240 min, followed by a slower adsorption phase. The adsorption equilibrium can be almost achieved within 24 h. Thus, an adsorption duration of 24 h was chosen to ensure the adsorption equilibrium in the following tests. By non-linear kinetics simulation, the simulated kinetics parameters for both biochars under different pH conditions are listed in Table 2. For both the as-prepared and demineralized BC200, the experimental points were much close to the simulated curves by the pseudo-second-order kinetics model. Further, their determined coefficients ( $R^2$ ) of the pseudo-second-order models were all above 0.950, which were much higher than those derived from the pseudo-first-order and Elovich models. Totally, the

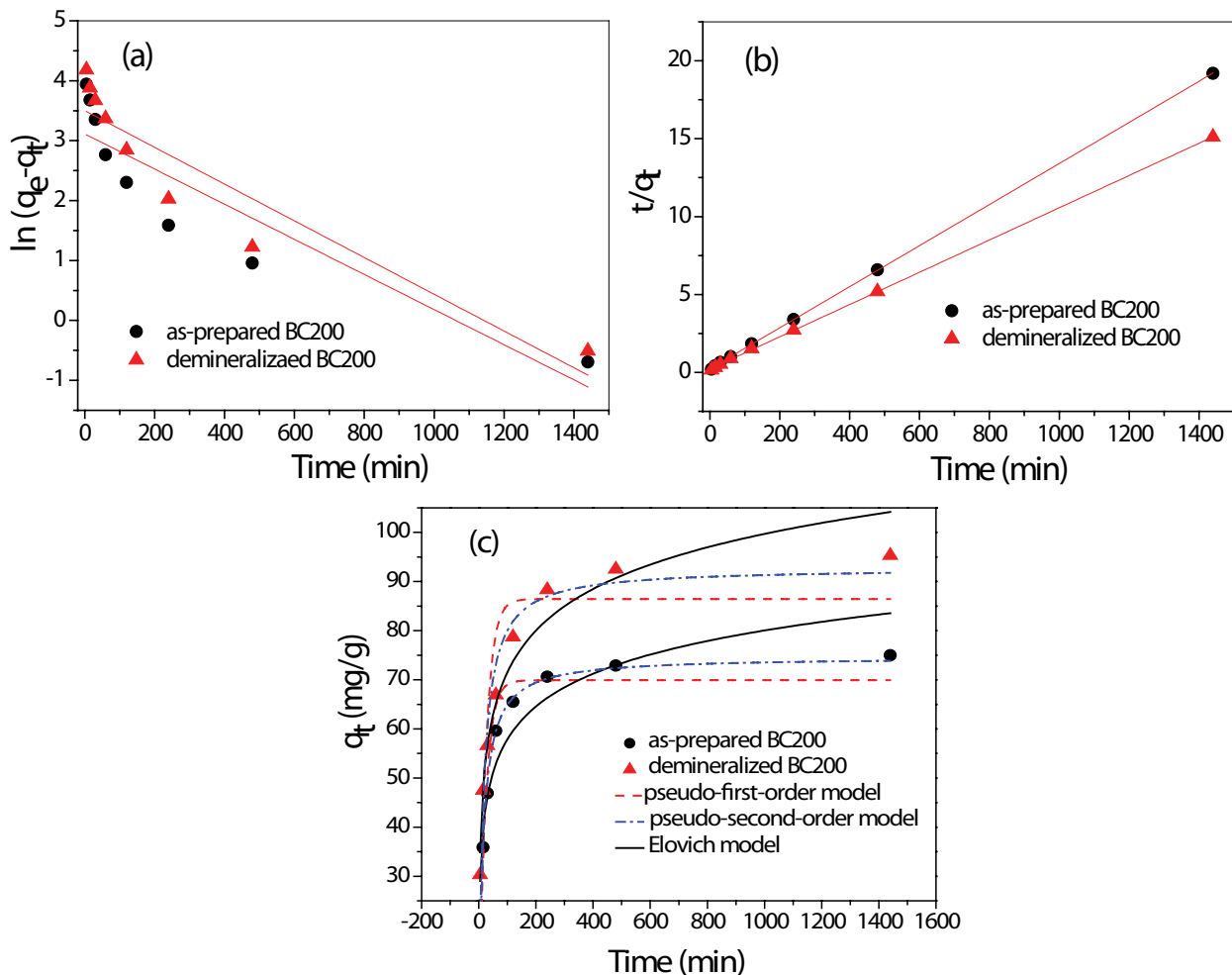


Fig. 6. Linear (a,b) and non-linear (c) adsorption kinetics for the pseudo-first-order (a), pseudo-second-order (b) and Elovich simulation for MB onto the biochar BC200 at neutral solution pH.

Table 1  
Linear kinetics parameters simulated by the pseudo-first-order and pseudo-second-order kinetic models for MB adsorption on both the as-prepared BC200 (BC200) and demineralized BC200 (D-BC200)

		Linear pseudo-first-order model			Linear pseudo-second-order model		
		$q_e$ (mg/g)	$k_1$ (min <sup>-1</sup> )	$R^2$	$q_e$ (mg/g)	$k_2$ (mg/(g min))	$R^2$
BC200	pH = 3	20.27	$0.2 \times 10^{-3}$	0.901	12.59	$1.59 \times 10^{-3}$	0.960
	pH = 5	39.44	$3.02 \times 10^{-3}$	0.903	76.69	$0.27 \times 10^{-3}$	0.999
	pH = 7	22.48	$2.93 \times 10^{-3}$	0.807	75.82	$0.79 \times 10^{-3}$	0.999
	pH = 9	20.94	$2.64 \times 10^{-3}$	0.785	72.20	$0.85 \times 10^{-3}$	0.999
	pH = 11	10.42	$2.18 \times 10^{-3}$	0.557	92.94	$2.32 \times 10^{-3}$	0.999
D-BC200	pH = 3	4.11	$1.35 \times 10^{-3}$	0.804	6.40	$2.55 \times 10^{-3}$	0.998
	pH = 5	41.3	$3.04 \times 10^{-3}$	0.981	56.37	$0.21 \times 10^{-3}$	0.993
	pH = 7	33.2	$3.07 \times 10^{-3}$	0.858	96.62	$0.503 \times 10^{-3}$	0.999
	pH = 9	25.3	$2.91 \times 10^{-3}$	0.685	96.81	$0.67 \times 10^{-3}$	0.999
	pH = 11	2.00	$1.26 \times 10^{-3}$	0.036	95.51	$2.60 \times 10^{-3}$	0.999

Table 2  
Non-linear kinetics parameters simulated by the pseudo-first-order, pseudo-second-order and Elovich models for MB adsorption on both the as-prepared BC200 (BC200) and demineralized BC200 (D-BC200)

Pseudo-first-order model	BC200			D-BC200		
Pseudo-first-order	$q_e$ (mg/g)	$k_1$ (min <sup>-1</sup> )	$R^2$	$q_e$ (mg/g)	$k_1$ (min <sup>-1</sup> )	$R^2$
pH = 3	11.09	$1.03 \times 10^{-2}$	0.949	5.37	$1.8 \times 10^{-2}$	0.937
pH = 5	69.06	$1.63 \times 10^{-2}$	0.972	46.44	$1.1 \times 10^{-2}$	0.915
pH = 7	69.90	$4.37 \times 10^{-2}$	0.902	86.45	$4.2 \times 10^{-2}$	0.817
pH = 9	66.08	$4.88 \times 10^{-2}$	0.831	89.77	$4.3 \times 10^{-2}$	0.885
pH = 11	88.43	$1.54 \times 10^{-1}$	0.870	94.8	$2.86 \times 10^{-1}$	0.956
Pseudo-second-order	$q_e$ (mg/g)	$k_2$ (mg/(g min))	$R^2$	$q_e$ (mg/g)	$k_2$ (mg/(g min))	$R^2$
pH = 3	12.70	$1.0 \times 10^{-3}$	0.976	6.01	$4.0 \times 10^{-3}$	0.986
pH = 5	76.49	$3.0 \times 10^{-4}$	0.998	52.94	$3.0 \times 10^{-4}$	0.969
pH = 7	74.64	$9.0 \times 10^{-4}$	0.981	92.77	6.771	0.951
pH = 9	70.20	$1.1 \times 10^{-3}$	0.952	96.05	$7.0 \times 10^{-4}$	0.972
pH = 11	92.39	$2.0 \times 10^{-3}$	0.997	96.97	$6.0 \times 10^{-3}$	0.964
Elovich	$a$ (g mg/min) (g mg/min)	$k$ (mg/g)	$R^2$	$a$ (g mg/min)	$k$ (mg/g)	$R^2$
pH = 3	-4.27	2.37	0.986	0.983	-1.01	1.03
pH = 5	-12.50	12.98	0.964	0.976	-11.34	8.86
pH = 7	13.57	9.62	0.901	0.949	15.17	12.24
pH = 9	16.31	8.57	0.913	0.898	17.13	12.41
pH = 11	53.79	6.42	0.726	0.456	77.8	3.11

pseudo-second-order kinetic model was better to describe the adsorption kinetics, suggesting possible chemisorption occurring between MB molecules and biochars.

### 3.6. Adsorption isotherm

Adsorption isotherm study for MB uptake on both the as-prepared and demineralized BC200 was conducted at

three different reaction temperatures (288, 298 and 308 K). The isotherm curves of both biochars at 298 K are plotted in Fig. 7. The Langmuir and Freundlich models were employed to fit the experimental data.

The Langmuir equation is represented as [25]:

$$q_e = \frac{q_m k_L C_e}{1 + k_L C_e} \tag{9}$$

The Freundlich equation is represented as [26]:

$$q_e = k_f C_e^{\frac{1}{n}} \quad (10)$$

where  $q_e$  is the amount of MB adsorbed onto the sludge biochar (mg/g),  $C_e$  is the equilibrium concentration (mg/L),  $q_m$  is the maximum adsorption capacity of the sludge biochar (mg/g),  $k_L$  is the equilibrium adsorption constant related to the affinity of binding site (L/mg),  $k_f$  is the Freundlich constants related to the adsorption capacity.

The fitted isotherm curves are shown in Fig. 7 and the isotherm parameters are given in Table 3. Based on the determined coefficient listed in Table 3, the Langmuir model fitted the experimental data better than the Freundlich model. Similarly, the determined coefficients ( $R^2$ ) of Langmuir model were all higher than those of Freundlich model at all the temperatures. The fitting results indicated that the monolayer coverage of MB occurred on both biochars. Additionally, at 298 K, the maximum adsorption capacities

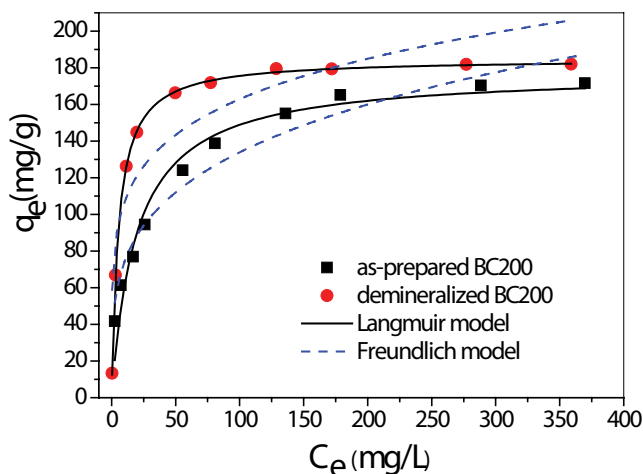


Fig. 7. Adsorption isotherms for MB on both the as-prepared and demineralized BC200 at 298 K.

Table 3  
Langmuir and Freundlich isotherm parameters for the adsorption of MB onto both the as-prepared (BC200) and demineralized BC200 (D-BC200)

	BC200			D-BC200		
	288 K	298 K	308 K	288 K	298 K	308 K
Langmuir						
$q_m$ (mg/g)	151.2	177.6	247.4	151.1	184.9	241.1
$k_L$ (L/mg)	0.045	0.051	0.050	0.35	0.19	0.21
$R^2$	0.984	0.955	0.956	0.999	0.999	0.988
Freundlich						
$k_f$ (mg/g)	31.5	41.0	57.0	72.0	69.9	94.7
$n$	3.57	3.89	3.92	7.01	5.45	5.57
$R^2$	0.939	0.951	0.919	0.753	0.815	0.839

Table 4  
Comparison of MB adsorption capacities on various carbonaceous sorbents

Sorbents	$q_m$ (mg/g)	Solution pH	References
Sludge biochar BC200	177.6	7.0	This study
Demineralized BC200	184.9	7.0	This study
Demineralized anaerobic			
Sludge BC650	90.91	N.A.	[12]
Sludge BC550	24.1	N.A.	[17]
Wheat straw BC200	46.6	7.0	[15]
Carbon nanotubes	188.68	6.0	[27]
Graphene oxide	243.9	6.0	[27]
Activated carbon	270.27	6.0	[27]
Activated sludge	66.23	N.A.	[28]
Anaerobic digestion residue	9.5	N.A.	[29]
Palm bark	2.66	N.A.	[29]
Eucalyptus	2.06	N.A.	[29]
Phoenix tree leaves	80.9	N.A.	[30]
Pistachio hull waste	389	8.0	[31]

<sup>a</sup>N.A. = Not available

<sup>b</sup>Suffix of BC indicates the pyrolytic temperature for biochar

( $q_m$ ) calculated from the Langmuir model for the as-prepared and demineralized BC200 were 177.6 and 184.9 mg/g, respectively. The increasing reaction temperature can improve the adsorption capacity of MB on both biochars, suggesting that the adsorption process was endothermic process. The adsorption capacities of other carbonaceous sorbents reported for MB uptake in literature are compared in Table 4. The as-prepared and demineralized BC200 outperformed other biochars although their  $q_m$  are lower than those of carbon nanotubes, graphene oxide and activated carbon.

#### 4. Conclusion

Low-temperature sludge biochar was prepared by pyrolyzing municipal waste activated sludge and used for the adsorptive removal of MB. The sludge biochar pyrolyzed at 200°C (BC200) outperformed the biochars prepared at other temperatures. The sophisticated pore structure and suitable surface properties of sludge biochar might facilitate the uptake of MB, in which the surface functional groups played the key role. The uptake of MB on the as-prepared BC200 increased with the increase of pH, while the optimal adsorption of MB can be achieved at pH 7.0 for the demineralized BC200. The pseudo-second-order kinetic model fitted the experimental data better. The Langmuir model did a better job on the fitting of the experimental data than the Freundlich model, indicating monolayer coverage of MB occurred on both biochars. At 298 K, the calculated maximum adsorption capacities ( $q_m$ ) of the demineralized BC200 were slightly higher than that of the as-prepared BC200. Both BC200 biochars outperformed other biochars previously reported in the literature.

## Acknowledgements

The authors thank for the financial supports from the National Natural Science Foundation of China (Grant No. 51378205) and the Natural Science Foundation of Henan Province (Grant No.182300410136).

## References

- [1] J.H. Qu, Research progress of novel adsorption processes in water purification, *J. Environ. Sci.*, 20 (2008) 1–13.
- [2] I. Ali, M. Asim, T.A. Khan, Low cost adsorbents for the removal of organic pollutants from wastewater, *J. Environ. Manage.*, 113 (2012) 170–183.
- [3] L. Wang, G.C. Chen, C. Ling, J.F. Zhang, K. Szerlag, Adsorption of ciprofloxacin on to bamboo charcoal: effects of pH, salinity, cations, and phosphate, *Environ. Prog. Sustainable*, 36 (2017) 1108–1115.
- [4] M. Rafatullah, O. Sulaiman, R. Hashim, A. Ahmad, Adsorption of methylene blue on low-cost adsorbents: a review, *J. Hazard. Mater.*, 177 (2010) 70–80.
- [5] M. Ahmad, A.U. Rajapaksha, J.E. Lim, M. Zhang, N. Bolan, D. Mohan, M. Vithanage, S.S. Lee, Y.S. Ok, Biochar as a sorbent for contaminant management in soil and water: a review, *Chemosphere*, 99 (2014) 19–33.
- [6] D. Mohan, A. Sarswat, Y.S. Ok, C.U. Pittman Jr., Organic and inorganic contaminants removal from water with biochar, a renewable, low cost and sustainable adsorbent – a critical review, *Bioresour. Technol.*, 160 (2014) 191–202.
- [7] A.U. Rajapaksha, S.S. Chen, D.C.W. Tsang, M. Zhang, M. Vithanage, S. Mandal, B. Gao, N.S. Bolan, Y.S. Ok., Engineered/designer biochar for contaminant removal/immobilization from soil and water: potential and implication of biochar modification, *Chemosphere*, 148 (2016) 276–291.
- [8] G.T. Li, Y.P. Guo, W.G. Zhao, Efficient adsorption removal of tetracycline by layered carbon particles prepared from seaweed biomass, *Environ. Prog. Sustainable*, 36 (2017) 59–65.
- [9] J. Lehmann, A handful of carbon, *Nature*, 447 (2007) 143–144.
- [10] J.W. Lee, B. Hawkins, D.M. Day, D.C. Reicosky, Sustainability: the capacity of smokeless biomass pyrolysis for energy production, global carbon capture and sequestration, *Energy Environ. Sci.*, 3 (2010) 1695–1705.
- [11] M. Keiluweit, P.S. Nico, M.G. Johnson, M. Kleber, Dynamic molecular structure of plant biomass-derived black carbon (biochar), *Environ. Sci. Technol.*, 44 (2010) 1247–1253.
- [12] L. Shi, G. Zhang, D. Wei, T. Yan, X.D. Xue, S.S. Shi, Q. Wei, Preparation and utilization of anaerobic granular sludge-based biochar for the adsorption of methylene blue from aqueous solutions, *J. Mol. Liq.*, 198 (2014) 334–340.
- [13] Q.Y. Xu, S.Q. Tang, J.C. Wang, J.H. Ko, Pyrolysis kinetics of sewage sludge and its biochar characteristics, *Process Saf. Environ.*, 115 (2018) 49–56.
- [14] G.F. Song, Y.J. Guo, G.T. Li, W.G. Zhao, Y. Yu, Comparison for adsorption of tetracycline and cefradine using biochar derived from seaweed *Sargassum* sp., *Desal. Water Treat.*, 160 (2019) 316–324.
- [15] G.T. Li, W.Y. Zhu, C.Y. Zhang, S. Zhang, L.L. Liu, L.F. Zhu, W.G. Zhao, Effect of a magnetic field on the adsorptive removal of methylene blue onto wheat straw biochar, *Bioresour. Technol.*, 206 (2016) 16–22.
- [16] G.T. Li, W.Y. Zhu, L.F. Zhu, X.Q. Chai, Effect of pyrolytic temperature on the adsorptive removal of p-benzoquinone, tetracycline, and polyvinyl alcohol by the biochars from sugarcane bagasse, *Korean J. Chem. Eng.*, 33 (2016) 2215–2221.
- [17] S.S. Fan, Y. Wang, Z. Wang, J. Tang, J. Tang, X.D. Li, Removal of methylene blue from aqueous solution by sewage sludge-derived biochar: adsorption kinetics, equilibrium, thermodynamics and mechanism, *J. Environ. Chem. Eng.*, 5 (2017) 601–611.
- [18] H.R. Yuan, T. Lu, H.Y. Huang, D.D. Zhao, N. Kobayashi, Y. Chen, Influence of pyrolysis temperature on physical and chemical properties of biochar made from sewage sludge, *J. Anal. Appl. Pyrolysis*, 112 (2015) 284–289.
- [19] B. Chen, D. Zhou, L. Zhu, Transitional adsorption and partition on nonpolar and polar aromatic contaminants by biochars of pine needles with different pyrolytic temperatures, *Environ. Sci. Technol.*, 42 (2008) 5137–5143.
- [20] M.M. Mian, G. Liu, Sewage sludge-derived TiO<sub>2</sub>/Fe/Fe<sub>3</sub>C-biochar composite as an efficient heterogeneous catalyst for degradation of methylene blue, *Chemosphere*, 215 (2019) 101–114.
- [21] M. Kithome, J.W. Paul, L.M. Lavkulich, A.A. Bomke, Kinetics of ammonium adsorption and desorption by the natural zeolite clinoptilolite, *Soil Sci. Soc. Am. J.*, 62 (1988) 622–629.
- [22] C.W. Cheung, J.F. Porter, G. McKay, Sorption kinetics for the removal of copper and zinc from effluents using bone char, *Sep. Purif. Technol.*, 19 (2000) 55–64.
- [23] S. Lagergren, Zur theorie der sogenannten adsorption gelöster stoffe, *Kungliga Svenska Vetenskapsakademiens, Handlinga*, 24 (1898) 1–39.
- [24] Y.S. Ho, G. McKay, Pseudo-second-order model for sorption process, *Process Biochem.*, 34 (1999) 451–65.
- [25] I. Langmuir, Kinetic model for the sorption of dye aqueous solution by clay-wood sawdust mixture, *J. Am. Chem. Soc.*, 38 (1916) 2221–2295.
- [26] H.M.F. Freundlich, Über die adsorption in lasungen, *J. Phys. Chem.*, 57 (1906) 385–470.
- [27] Y.H. Li, Q.J. Du, T.H. Liu, X.J. Peng, J.J. Wang, J.K. Sun, Y.H. Wang, S.L. Wu, Z.H. Wang, Y.Z. Xia, L.H. Xia, Comparative study of methylene blue dye adsorption onto activated carbon, graphene oxide, and carbon nanotubes, *Chem. Eng. Res. Des.*, 91 (2013) 361–368.
- [28] K. Gobi, M.D. Mashitah, V.M. Vadivelu, Adsorptive removal of Methylene Blue using novel adsorbent from palm oil mill effluent waste activated sludge: equilibrium, thermodynamics and kinetic studies, *Chem. Eng. J.*, 171 (2011) 1246–1252.
- [29] L. Sun, S.G. Wan, W.S. Luo, Biochars prepared from anaerobic digestion residue, palm bark, and eucalyptus for adsorption of cationic methylene blue dye: characterization, equilibrium, and kinetic studies, *Bioresour. Technol.*, 140 (2013) 406–413.
- [30] R.P. Han, W.H. Zou, W.H. Yu, S.J. Cheng, Y.F. Wang, J. Shi, Biosorption of methylene blue from aqueous solution by fallen phoenix tree's leaves, *J. Hazard. Mater.*, 141 (2007) 156–162.
- [31] G. Moussavi, R. Khosravi, The removal of cationic dyes from aqueous solutions by adsorption onto pistachio hull waste, *Chem. Eng. Res. Des.*, 89 (2011) 2182–2189.